Prediction of CO_2 Mass Transfer Flux in Aqueous Amine Solutions Using Artificial Neural Networks

Ghaemi, Ahad*+; Jafari, Zahra; Etema, Edris

School of Chemical, Petroleum and Gas Engineering, Iran University of Science and Technology, P.O. Box 16765-163, Tehran, I.R. IRAN

ABSTRACT: *In the present research, neural networks were applied to predict mass transfer flux of CO_2 in aqueous amine solutions. Buckingham π theorem was used to determine the effective dimensionless parameters on CO_2 mass transfer flux in reactive separation processes. The dimensionless parameters including CO_2 loading, the ratio of CO_2 diffusion coefficient of gas to a liquid, the ratio of the CO_2 partial pressure to the total pressure, the ratio of film thickness of gas to liquid and film parameter as input variables and mass transfer flux of CO_2 as output variables were in the modeling. A multilayer perceptron network was used in the prediction of CO_2 mass transfer flux. As a case study, experimental data of CO_2 absorption into Piperazine solutions were used in the learning, testing, and evaluating steps of the multilayer perceptron. The optimal structure of the multilayer perceptron contains 21 and 17 neurons in two hidden layers. The predicting results of the network indicated that the mean square error for mass transfer flux was 4.48%. In addition, the results of the multilayer perceptron were compared with the predictions of other researchers' results. The findings revealed that the artificial neural network computes the mass transfer flux of CO_2 more accurately and more quickly.*

KEYWORDS: *Prediction; Absorption; Mass transfer Flux; CO_2, Piperazine; Multilayer Perceptron.*

INTRODUCTION

CO_2 is one of the most important greenhouse gases which are mainly produced by chemical material and industrial units. Due to environmental issues, CO_2 which is released from chemical material should be reduced and controlled. A variety of technologies for CO_2 eliminating are developed and proposed. These methods are considered highly practical and efficient in their function by using absorption process with chemical reactions [1]. The technological process of getting rid of CO_2 based on amine solution is considered as the most effective and frequently used economic method of diminishing CO_2. CO_2 absorption in amine solutions forms carbamate or bicarbonate. Absorption rate depends on physical and chemical characteristics of amine solutions and the operational conditions of the process including temperature and partial pressure of CO_2, amine concentration. In the recent years, the researchers have suggested a variety of amines to eliminate CO_2. *Norouzbahari et al.* [2], *Hartono et al.* [3], *Paul et al.* [4], *Sema et al.* [5], *Naami et al.* [6], *Porcheron et al.* [7] have proposed amines with different capabilities. One of the solvents which have been recently recognized is

** To whom correspondence should be addressed.*
+ E-mail: aghaemi@iust.ac.ir
1021-9986/2020/4/269-280 12/$/6.02

Table 1: Reaction rate constant of some amines with CO_2 [8].

Amine type	)lit/mol.s(Reaction rate constant
MDEA	4
DIPA	100
DEA	1300
DGA	4500
MMEA	7100
MEA	6000
Pz	59000

Piperazine (Pz) solution. This primary amine which has annular structure and because of its chemical structure has a very high reaction rate and this feature has attracted many interests and attentions. Due to the high reaction rate of Pz, this solvent is recently used as a promoter for solvents having lower rate. In Table 1, reaction rate constant of some common amines with CO_2 is presented.

Table 1 indicates that the reaction rate constant of Pz compared to MDEA, which is highly common, is much greater. Moreover, the volatility of this solvent in the temperature of 40 ^oC is between 10-19 ppm and its thermal decomposition is negligible up to 150^oC [9]. However, the most important issue in CO_2 absorption is computing the mass transfer flux. In the absorption processes, the absorption operation is performed in the form of either physical absorption or absorption with chemical reaction. To compute the mass transfer flux in chemical absorption, the effect of chemical reaction on the mass transfer is performed by enhancement factor. The enhancement factor is ratio of mass transfer flux from interface in a reaction condition to the condition without any reaction and the hydrodynamic and driving force in both conditions are similar. In other words, enhancement factor considers the effect of chemical reactions of carbon dioxide mass transfer [10].

Enhancement factor is based on reaction rate and it can be proposed to be different, larger or equal to one. The most important discussion in this regard is finding the precise relation of the enhancement factor. Since this factor follows other parameters, it is evident that as the complexity of the reaction and process increases proposing a relation for the enhancement factor can be more complex and difficult as well. A variety of relations for calculating enhancement factor are proposed and each of them is only relevant to a specific issue and none of them is precise enough. Researchers such as *Van Krevelens* [11-12], *Decoursey* [13-14-15], *Shen* [16], *Stichlmair* [17] and *Mamun* [18] have proposed different relations for enhancement factor based on the film model as follow:

$$N_{CO_2} = Ek_l\left(C_{CO_2,i} - C_{CO_2,b}\right)$$

The summarized enhancement factors are presented in Table 2. These relations are for specific situations and in order to reach to the available factors, different simplifications in boundary conditions are conducted and this causes error in computing mass transfer flux. A more important issue is that in using enhancement factor only one main reaction is considered and the effect of other reactions is ignored. For example, in the reaction of CO_2 in amines, reactions of CO_2 with water and hydroxide ion are not taken into consideration. There are different reactions in the absorption system of CO_2 with Piperazine solution which increases mass transfer of CO_2 and if enhancement factor in computing mass transfer flux is used, a huge error will occur. Therefore, in this research, in order to apply effect of all reactions, film parameter has been employed.

In some cases, some correlations were presented based on mass transfer parameters for computing mass transfer flux. Table 3 shows mass transfer correlations for reactive separation processes. These correlations are limited to operation conditions that used to determine the correlation constant. Therefore they cannot applicable for wide range of operating conditions.

By presenting the disadvantages of enhancement factor method and correlations, the use of a more practical and precise method seems indispensable and it is due to the fact that by accurately computing mass transfer flux, dimensions of absorption column can be computed precisely.

The development of numerical tools, such as Artificial Neural Network (ANN), has paved the way for alternative methods to predict the chemical processes parameters especially thermodynamic, mass transfer and hydrodynamic parameters [28-31]. Yehia and Elshazly used neural networks to estimate mass transfer coefficient from the bottom of agitated vessel [28]. *Adnan et al.* applied artificial neural network in the calculation of the thermodynamic properties of an alternative refrigerant [32]. *Jouyban et al.* investigated the solubility prediction

Table 2: Enhancement factors for chemical absorption processes.

Enhancement factor	Reaction	References
$E_A = \frac{Ha}{\tanh(Ha)}(1 - \frac{C_{A,b}}{C_{A,i}}\frac{1}{\cosh(Ha)})$	First order and pseudo first order $A \rightarrow P$	[19]
$E_A = \left(1 + \frac{a}{b}\frac{D_B}{D_A}\frac{C_{B,b}}{C_{A,i}}\right)$	Irreversible second order $aA+bB \rightarrow P$	[20]
$E_A = \frac{Ha}{\tanh(Ha)}(1 - \frac{C_{A,b}}{C_{A,i}}\frac{1}{\cosh(Ha)})$	Irreversible second order $\gamma_A A \rightarrow P$	[21]
$E_A = \frac{1+K}{1+\frac{K\tanh\beta}{\beta}}, \beta - \frac{\sqrt{D_A k_1 (K+1)/K}}{k_L}$	Reversible first order $A \leftarrow \frac{k_1}{k_{-1}} \rightarrow E$	[22]
$E_A = 1 + \left(\frac{D_B}{D_A}\right)\frac{C_{B,b}}{C_{A,i} + \frac{D_B/D_E}{K}}$	Reversible first order $A \leftarrow \frac{k}{k_{-1}} \rightarrow 2E$	[22]
$E_A = \left(1 - \frac{C_{A,b}}{C_{A,i}}\right)\left(1 + \frac{P+1}{m+1}\frac{D_E/D_A}{\gamma_E/\gamma_A T}\right) + \frac{\frac{D_E/D_A}{\gamma_E/\gamma_A}\left(\frac{P+1}{m+1}\frac{C_{A,b}/C_{A,i}}{T} - \frac{C_{E,b}}{C_{A,i}}\right)\left(1 - \frac{1}{\cosh\sqrt{M}}\right)}{1 + \frac{P+1}{m+1}\frac{D_E/D_A}{\gamma_E/\gamma_A T}\frac{\tanh\sqrt{M}}{\sqrt{M}}}$	Reversible second order $A + B \leftarrow \frac{k_1}{k_{-1}} \rightarrow E + F$	[23]
$E_A = 1 + \frac{1}{n}\frac{D_B}{D_A}\frac{C_{B,b}}{C_{A,i}}\frac{\frac{C_{B,i}}{C_{B,b}}}{1 - \frac{C_{A,b}}{C_{A,i}}}$	Reversible second order $A + B \leftarrow \frac{k_1}{k_{-1}} \rightarrow E$	[24]

Table 3: Mass transfer correlations.

$N_{CO2} = K_L \times CR^{-0.0087} \times M^{0.894}([CO_2]^* - [CO_2]_e)$	[25]
$N_{CO_2} = 1.37 \times K_L^0 \times \left(\alpha_{CO2,i}\right)^{0.17} \times (Ha)^{0.90} \times ([CO_2]_i - [CO_2]_b)$	[26]
$N_{CO_2} = K_L(CO_2^* - CO_{2b})(\alpha)^{-1.2407} \cdot \left(\frac{P_{CO_2}}{P_t}\right)^{0.8622} \left(\frac{\delta_g}{\delta_L}\right)^{-0.7206} \left(\frac{D_g}{D_L}\right)^{3.2883} (M)^{-0.6864}$	[27]

of anthracene in binary and ternary solvents using artificial neural networks [33].

ANN offers nonlinear mapping capability that can be applied for storage and recollection of mass transfer data [28]. The associative property of artificial neural networks and their inherent ability to learn and recognize highly non-linear finds them ideally suited to a wide range of applications in the chemical engineering processes. Many different types of neural networks have been developed [33-35]. The MultiLayer Perceptron (MLP) and radial basis function (RBF) are the most popular networks in the chemical engineering applications. They have been widely used for estimation of chemical processes variables. They are both non-linear feed-forward networks and universal approximators. MLPs are usually trained with the back-propagation supervised algorithm, whereas RBF networks are usually trained one layer at a time with the first layer unsupervised [33-35].

Accordingly, in the current research, neural networks were used for precisely computing the mass transfer flux of CO_2. In this work, both liquid and gas phases mass

transfer variables were used in the neural network models.

Based on the fast development and the widespread success of applying artificial neural networks in different aspects of science and engineering, a model based on ANN can be an appropriate substitution for overcoming the constraints and complexities of a process. In addition, some attention has been directed towards its capability in solving linear and non-linear problems [28].

THEORITICAL SECTION

Mass transfer flux variables

In computing mass transfer flux of CO_2 in amine solutions, the following variables are included in the process: partial pressure, total pressure, diffusion coefficient of components in phases, concentration of components in solution, rates of chemical reactions in solution and mass transfer coefficient.

$$N_{CO_2} = f\left(k, k_L, D_G, D_L, \delta_G, \delta_L, P_{CO_2}, P_t, C_{CO_2}, C_{AM}\right) \quad (1)$$

Dimensionless variables in absorption process are derived using the Buckingham theorem based on the following formula [27]:

$$\frac{N_{CO_2}}{k_l(C^*_{CO_2} - C_{CO_2,b})} = f\left(\frac{P_{CO_2}}{P}, \frac{D_g}{D_l}, \frac{\delta_g}{\delta_l}, M, \alpha\right) \quad (2)$$

These variables, which are dimensionless numbers in the process, are effective in computing mass transfer flux. Since in the above formula N_{CO2} should be computed, the input variables of the neural networks are presented in Table 4.

Case study: CO_2 absorption into piperazine solution

Where, α denotes the CO_2 loading in the solution which expressed as total moles of CO_2 absorbed both chemically and physically per mole of amine. It's defined as follows [36].

$$\alpha = \frac{C_{CO_2}}{C_{pz}} \quad (3)$$

This parameter is indicative of the effect of the concentration of components and if this parameter is lower, mass transfer driving force is higher and therefore the extent of absorption becomes higher; and in larger amounts, the amount of absorption decreases. The overall Pz solution and CO_2 concentration balance are as follow:

$$C_{PZ} = m_{PZ} + m_{PZH^+} + m_{PZH_2^{2+}} + m_{PZCOO} + m_{PZH(COO^-)_2} + m_{PZH^+COO^-} \quad (4)$$

$$C_{CO_2} = m_{CO_2} + m_{HCO_3^-} + m_{CO_3^{-2}} + m_{PZCOO^-} + 2m_{PZH(COO^-)_2} + m_{PZH^+COO^-} \quad (5)$$

For computing the concentration of ionic and molecular components, all the required equations must be considered. These equations include: charge balance equation, reaction constant equations and balance equations for amine and CO_2. These two equations are necessary for computing the concentrations of components after reaction. In addition to the equilibrium equations, overall Pz and CO_2 concentrations as well as charge balance must be satisfied. Charge balance equation is as follows:

$$m_{H^+} + m_{PzH^+} + 2m_{PzH_2^{2+}} = m_{OH^-} + m_{HCO_3^-} + 2m_{CO_3^{2-}} + m_{PzCOO^-} + 2m_{Pz(COO^-)_2} \quad (6)$$

Solving this set of independent equations for a given temperature, Pz overall concentration, and CO_2 loading results in the true (equilibrium) composition of the liquid phase, expressed as the molality of each species (mol/kg), needed for solving the VLE equations.

In this work, activity coefficients of both molecular and ionic species were calculated using the modified Pitzer's thermodynamic model for the excess Gibbs energy of aqueous electrolyte solutions. This form is as follows:

$$\frac{G^E}{RTn_wM_w} = f_1(I) + \sum_{i\neq w}\sum_{j\neq w} m_i m_j \lambda_{ij}(I) + \sum_{i\neq w}\sum_{j\neq w}\sum_{k\neq w} m_i m_j m_k \tau_{ijk} \quad (7)$$

Where $f_1(I)$ is modified Debye-Huckel term and M_w is molar mass of water.

The parameters of pitzer equation include: β_{ij}: binary interaction parameter between species i and j, λ_{ij}: second virial coefficient, τ_{ijk}: ternary interaction parameter.

M is considered as the Film parameter and is used for considering the effect of chemical reactions in mass transfer [37].

$$M^2 = \frac{D_l \times \sum_{i=1}^{4} r_{i,CO_2}}{k_1^2 [CO_2]^*} \quad (8)$$

Table 4: Dimensionless parameters obtained from Buckingham π theorem.

Number	Concept and definition	Dimensionless number
1	Enhancement factor: the ratio of the absorption rate of a gas into a reacting liquid to that if there was no reaction	$E = \frac{N_{CO_2}}{k_L \left(C^*_{CO_2} - C_{CO_2,b}\right)}$
2	Sherwood: indicative of the ratio of convection mass transfer to diffusion mass transfer	$Sh = \frac{k_L \delta_L}{D_L}$
3	Film conversion parameter: indicative of the ratio of maximum possible conversion in the film to maximum diffusional transport through the film	$M^2 = \frac{D_1 \times \sum_{i=1}^{n} r_{i,CO_2}}{k_l^2 [CO_2]^*}$
4	CO_2 loading: indicative of the ratio of moles CO_2 absorbed to moles amine circulating in process	$\alpha = \frac{C_{CO_2}}{C_{AM}}$
5	Films thickness ratio: Ratio of gas film thickness to liquid film thickness	$\frac{\delta_G}{\delta_L}$
6	CO_2 mole fraction: Ratio of CO_2 partial pressure to the total pressure	$\frac{P_{CO_2}}{P_t}$
7	Diffusion coefficients ratio: Ratio of diffusion coefficient in gas phase to liquid phase	$\frac{D_G}{D_L}$

The film parameter is used for applying the effect of chemical reactions in mass transfer. The film parameter is indicator of mass transfer regime. The magnitude of this number is the determiner of location of reaction and type of mass transfer device. As this number becomes larger, the location of conducting reaction moves towards the interface. Therefore, the reaction tents to be instantaneous. On the other hand, as this amount decreases, the location of conducting reaction moves towards the liquid bulk.

The reactions of Pz with CO_2 including: hydrolyze of mono-carbamate Piperazine [36].

$$CO_2 + PZ + H_2O \xleftarrow{k_1} PZCOO^- + H_3O^+ \quad (9)$$

Hydrolyze of dicarbamate Piperazine

$$CO_2 + PZCOO^- + H_2O \xleftarrow{k_2} PZ(COO^-)_2 + H_3O^+ \quad (10)$$

Formation of bicarbonate:

$$CO_2 + OH^- \xleftarrow{k_3} H_3CO^- \quad (11)$$

The reaction of water with CO_2:

$$CO_2 + H_2O \xleftarrow{k_4} H_3CO^- + H^+ \quad (12)$$

A wetted wall column contactor has been used to measure the experimental data [1]. The modeled threshold of operating conditions of absorption process which simulated is presented in Table 5.

Geometric design of the neural network

The basic and essential structure of a multi-layered (input, hidden and output layers) neural network is made up of neuron unit, which each one without having a connection with existing neurons in similar layers, is completely connected with neurons in neighboring layers. The neural network is modeled based on the human's neural system and, in fact, is an imitation of human's brain and neural network. In this network, the attempt is for creating a structure which similar to human brain has learning, generalization and decision-making power. In such structures the goal is introducing the operations of a dynamic system which is possible to train the model, store the way of system operates in the model and use it in cases where it has not been used previously. Because of the capability of such networks in modeling the highly complex processes in which the number of influential factors is highly abundant, its use in engineering applications is flourishing. The most important part of a neural network is neuron. The neurons are the constituting cells of human's neural system. Each neural network consists of input, hidden and output layers and in each layer there are one or more neurons. Each neurons of the input layer are multiplied in a weight whose amount determines the effect of each variable on the performance of each initial layer. Each neuron consists of two parts. In the first part, the sum of weight of initial material is computed. This mathematical function

Table 5: The operating conditions of CO_2 absorption in aqueous Pz [1].

Pz concentration (molality)	Loading (mol CO_2/mol amine)	CO_2 Partial pressure (pa)	Pressure (psig)	Temperature (°C)
2, 5, 8, 12	0.226 - 0.412	18 - 66330	20 - 70	40 - 100

is called transfer function whose performance is similar to a nonlinear filter and causes the output of neuron to be determined in a specific numerical range. The most important issue in the neural network models is the selection of appropriate input to the model in order to reach to an intended output. In addition, the structure of neural networks and the way of selecting relationship among neurons and the weight each neuron dedicate to itself are highly important. The structure of a neural network is consisted of number of layers, number of neurons in each layer, the way layers are connected to each other, training method of the network and the way parameters are distributed [38].

In the present work, in order to expand the ANN model for the purpose of mass transfer flux prediction (as output variable) (N_A), the effective parameters in the absorption process are selected as the input variables. Since the chemical absorption of CO_2 is exothermic process, the temperature increases in one column with the rise of reaction. Generally, the temperature directly affects the mass transfer and the efficiency of absorption process. In the current work, the temperature is not included in the neural network model. However, the effects of temperature on the efficiency of mass transfer on the basis of loading terms of amines, diffusion coefficient and film parameter are taken into consideration. These parameters change as temperature changes.

Four different training algorithms have been used to train and test the ANN including Error Back Propagation (EBP) with momentum, Scaled Conjugate Gradient (SCG), Levenberg-Marquardt (LM) and Bayesian Regulation back propagation (BR).In this work, LM approach is used in the training of the multilayer perceptron network. Fig. 1 shows that three-layered network was used to CO_2 mass transfer flux prediction. (Input layer, hidden layer and output layer). For statistical modeling, only one hidden layer is often satisfactory [39]. Therefore the performance of the model with a system with one hidden layer is studied, by varying the number of neurons. In order to ensure the homogeneity of the distribution of the input and output data, all data are normalized from 0-1. This method is one of the most conventional ways of pre-processing data especially in cases where variables have different orders of magnitude.

The tansing transfer function, which is continuous, derivational and increasingly homogeneous, is considered as the function between input-hidden layers and transfer function between hidden-output layers is Purelin function. In this research, among the total data (104), 70 data are randomly chosen for training the network and 34 data are used to test the performance of the trained network. The optimal structure of the network contains 21 and 17 neurons in input and hidden layers, respectively (with trial and error) and one neuron in outer layer corresponding to the single dependent variable with 500 epochs.

Transfer functions calculate a layer's output from its net input. Multiple layers of neurons with nonlinear transfer functions allow the network to learn nonlinear relationships between input and output vectors. The linear output layer (purelin) is most often used for function fitting (or nonlinear regression) problems. Sigmoid output neurons (logsig, tansig) are often used for pattern recognition problems (in which a decision is being made by the network). Therefore, in this problem purelin has been selected as transfer function of output layer. In the following, the equations of common functions in multi-layer networks are presented [40].

$$a = \mathrm{purelin}(n) = n \tag{13}$$

$$a = \mathrm{tansig}(n) = 2/(1+\exp(-2*n))-1 \tag{14}$$

$$a = \mathrm{logsig}(n) = 1/(1+\exp(-n)) \tag{15}$$

Mean square error (MSE) or mean absolute error (MAE) was used to obtain number of neurons in hidden layers in optimal network.

$$MAE = \frac{1}{N}\sum_{k=1}^{N}\left|(t(k)-a(k))\right| \tag{16}$$

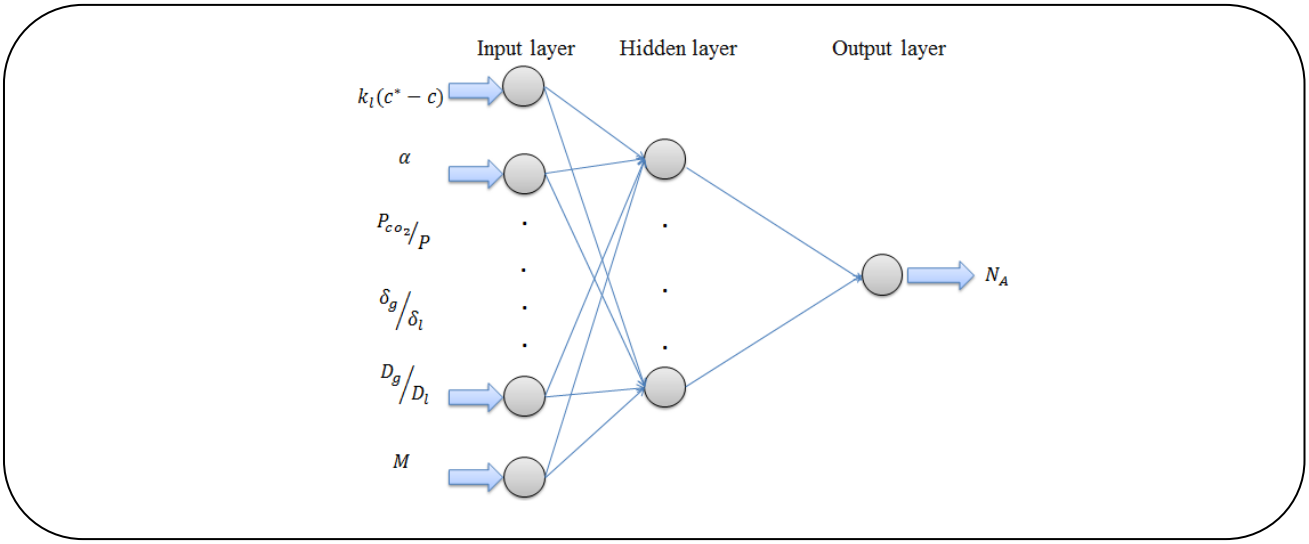

Fig. 1: Structure of the artificial neural network used for estimation of mass transfer flux: Connections between nodes are shown by solid lines.

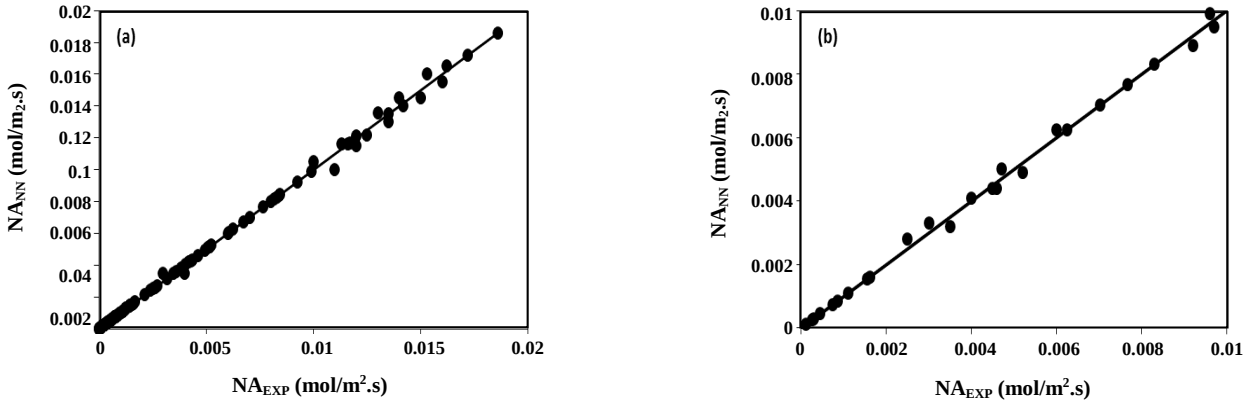

Fig. 2: ANN predictions versus experimental data of mass transfer flux: (a) for training set; (b) for testing set.

$$MSE = \frac{1}{N}\sum_{k=1}^{N} e(k)^2 = \frac{1}{N}\sum_{k=1}^{N} (t(k) - a(k))^2 \qquad (17)$$

Three criteria of time, mean square error and number of epochs were presented to stop neural networks. Mean square error is used to stop the network.

RESULTS AND DISCUSSION

Although ANN algorithm is a suitable tool to predict arbitrary variable in complex processes but it is essential to be well trained network, otherwise it is far away to have good estimation. Thus proper training is a prerequisite in network performance. Fig. 2 illustrates how the network has been trained and tested. As it is evident, the experimental values are in good agreement with the theoretical values, so a well-trained and well-tested network has been achieved.

As was previously mentioned, the modified Pitzer model is used to obtain the interfacial and liquid bulk concentration of molecular and ionic species. In Fig. 3, the changes in the amount of free Piperazine concentration in relation to the CO_2 loading are depicted. This figure shows that in a fixed concentration of the solution, as the loading extent decreases, the free Pz in the solution increases. This is due to the fact that as the loading in fixed concentration increases, the amount of absorbed CO_2 increases and this means that the mass transfer flux has increased. It is obvious that as extent

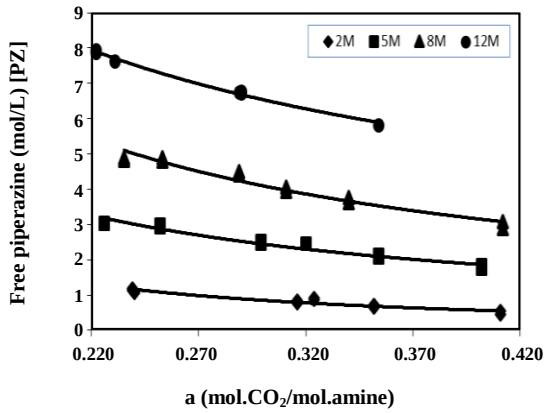

Fig. 3: Variation of free Piperazine in the solution with CO_2 loading.

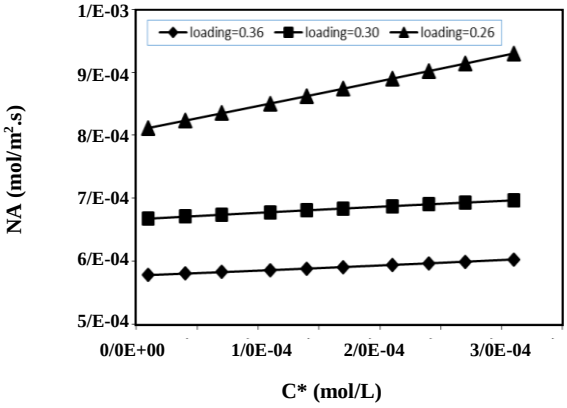

Fig. 4: The effect of the concentration of gas-liquid interface on the mass transfer flux.

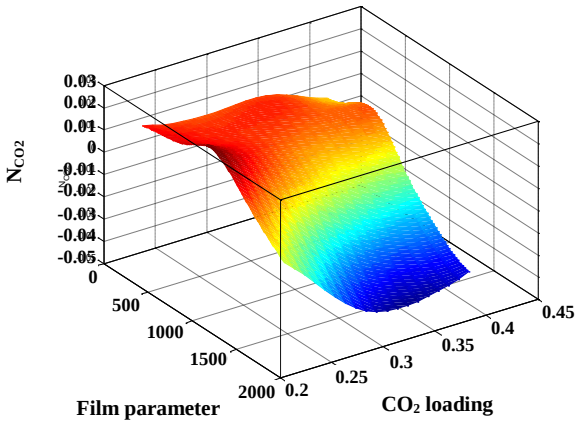

Fig. 5: Variation of CO_2 mass transfer flux with film parameter and CO_2 loading.

of flux increases, more Piperazine reacts, therefore free Pz decreases. The decreasing trend in the Fig. 3 shows this tendency. Moreover, it is observed that with an increase in the total concentration, more free Pz exist in the solution which is a natural issue.

In addition, the computed and analyzed mass transfer flux is used to measure and examine the efficiency and applications of the results obtained from the neural network model in different conditions of process. The relation between interfacial CO_2 concentration and mass transfer flux is depicted in Fig. 4. In this figure, the effect of loading and interfacial concentration in mass transfer flux is taken into consideration. As it is observed, the increase in the interfacial concentration is indicative of the increase in CO_2 absorption. This trend is highly evident in the ascending nature of the figure in which with an increase in the amount of loading in the single concentration of interface, mass transfer flux has decreased.

In Fig. 5, variation of CO_2 mass transfer flux with film parameter and CO_2 loading was presented. It is clear that CO_2 mass transfer was increased with increasing film parameter and decreasing CO_2 loading. In reactive absorption processes, film parameter present the effect of chemical reactions on mass transfer so, this figure indicates that chemical reactions was increased the mass transfer of CO_2 in the liquid phased.

Fig. 6 shows the relationship between the partial pressure of CO_2 in gas phase and the mass transfer flux. Naturally, in similar conditions, with an increase in the partial pressure of CO_2 in gas phase, more absorption and mass transfer flux can be achieved. The effect of loading is seen in the way that the increase in the loading of a fixed concentration of solution in a single and fixed mass transfer flux leads to an increase in the amount of absorbed CO_2 which is indicative of the increase in the partial pressure of CO_2 in gas phase. In fact, the increase in the partial pressure of CO_2 with an increase of loading in the amount of fixed flux is due to this fact.

Comparison of ANN results of mass transfer flux with experimental data was shown in Fig. 7. As it is observed, the amount of correlation coefficient (R^2) for the neural network is 0.986. However, the model of neural network for some data is undistinguishable. In other words, the complexities existing in the reaction types of piperazine, consideration of the existing parameters in an absorption

Table 6: The percentage of deviation in mass transfer flux computed using different methods.

Reference	Deviation (%)	References
Van Krevelen (1954)	12.00	[12]
Decoursey (1974)	12.00	[14]
Pangankar and M. M. Sharma (1974)	10.11	[41]
Shen et al. (1999)	14.90	[16]
Last and Stichlmair (2002)	10.00	[17]
Etemad et al. (2015)	5.80	[27]
Artificial Neural Network (ANN)	4.48	This work

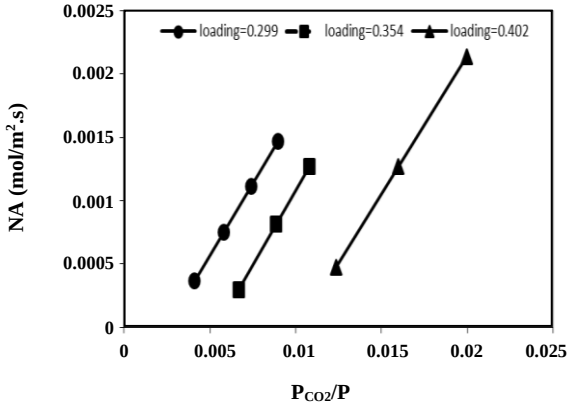

Fig. 6: The effect of partial pressure of CO_2 on the mass transfer flux.

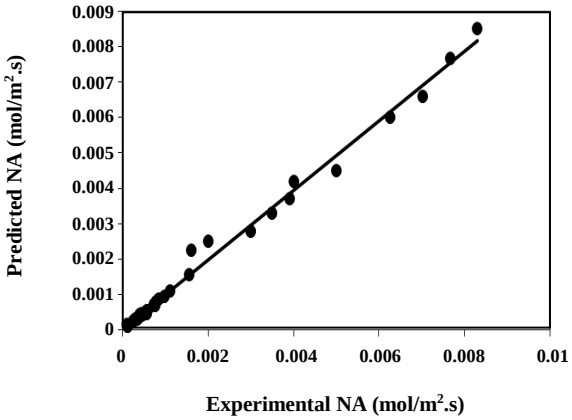

Fig. 7: Prediction of mass transfer flux by MLP neural network.

process and some other hypothesis in the thermodynamic model of the problem may cause further errors. The mean square error for neural network is 5.48% which indicates that the neural network has had acceptable results in mass transfer flux prediction.

In Table 6, the computed mass transfer flux in this research is compared with some other proposed methods based on the enhancement factor. As it is evident, the model of neural network has a smaller mean error compared to the other proposed relations.

CONCLUSIONS

In this work, mass transfer flux of CO_2 in Pz solution was investigated using multilayer neural network. The experimental data of CO_2 mass transfer flux presented in the literature were used to training and test of the neural network. The concentrations of equilibrium, ionic and molecular species were calculated applying modified Pitzer model. Input parameters of the neural network were obtained using Buckingham theorem. The effect of process parameters on mass transfer flux including CO_2 loading, concentration of Piperazine solution, film parameter were investigated. The increase in concentration of CO_2 in interface was the same as the amount of absorption which leads to an increase in the mass transfer flux. In addition, the increase of loading in a fixed concentration leads to decrease of free Piperazine in the solution. The results of neural network, despite the complexities of reaction, absorption process and considered hypothesis in computing the concentration of CO_2 in the liquid bulk and interface, are logical and acceptable results. The comparison between the experimental and predicted data indicates that the neural network is highly suitable for predicting the results of CO_2 absorption process and contains better and more precise results compared to the other mathematical

models and a variety of relations proposed in the literature.

Nomenclature

$C^{*}_{CO_2}$	Interfacial concentration of dissolved CO_2, mol/L
C_{CO_2}	Total carbon dioxide concentration, mol/L
$C_{CO_2,b}$	Molar concentration of CO_2 in liquid phase, mol/L
PZ	Total Piperazine concentration, mol/L
D_g	CO_2 diffusion coefficient in gas phase, m^2/s
D_l	CO_2 diffusion coefficient in liquid phase, m^2/s
E	Enhancement factor
k_l	Liquid side mass transfer coefficient, m/s
m_i	Concentration of species i, mol/kg
M	CO_2 film conversion parameter
N_{CO_2}	CO_2 absorption rate, $mol/m^2.s$
P	Total system pressure, psig
P_{CO_2}	Partial pressure of CO_2, Pa
r_{CO_2}	Overall CO_2 reaction rate, mol/L.s
α	CO_2 loading, mol/mol
δ_g	Gas film thickness, m
δ_l	Liquid film thickness, m

Received : Feb. 19, 2019 ; Accepted : Jun. 10, 2019

REFERENCES

[1] Goharrokhi M., Taghikhani V., Ghotbi C., Safekordi A., Najibi H., Correlation and Prediction of Solubility of CO_2 in Amine Aqueous Solutions, *Iran. J. Chem. Chem. Eng. (IJCCE)*, **29**(1): 111-124 (2010).

[2] Norouzbahari S, Shahhosseini Sh, Ghaemi A, Chemical Absorption of CO_2 Into an Aqueous Piperazine (PZ) Solution: Development and Validation of a Rigorous Dynamic Rate-Based Model, RSC Advances, **6** (46): 40017-40032 (2016).

[3] Hartono A., Silva E.F., Svendsen H.F., Kinetics of Carbon Dioxide Absorption In Aqueous Solution of Diethylene Triamine (DETA), *Chem. Eng. Sci.*, **64**: 3205-3213 (2009).

[4] Paul S., Ghoshal A.K., Mandal B., Kinetics of Absorption of Carbon Dioxide Into Aqueous Solution of 2-(1-Piperazinyl)-Ethylamine, *Chem. Eng. Sci.*, **64**: 313-321 (2009).

[5] Sema T., Naami A., Idem R., Tontiwachwuthikul P., Correlations for Equilibrium Solubility of Carbon Dioxide in Aqueous 4-(Diethylamino)-2-butanol Solutions, *Ind. Eng. Chem. Res.*, **50**: 14008-14015 (2011).

[6] Naami A., Edali M., Sema T., Idem R., Tontiwachwuthikul P., Mass Transfer Performance of CO_2 Absorption Into Aqueous Solutions of 4-(Diethylamino)-2-butanol, Monoethanolamine, and N-Methyldiethanolamine, *Ind. Eng. Chem. Res.*, **51**: 6470-6479 (2012).

[7] Porcheron F., Gibert A., Mougin P., Wender A., High Throughput Screening of CO_2 Solubility in Aqueous Monoamine Solutions, *Environ. Sci. Technol.*, **45**: 2486-2492 (2011).

[8] "Piperazine-Why It's Used and How It Works", Optimized Gas Treating Inc. (2008).

[9] Mondal M. K., Balsora H. K., Varshney P., Progress and Trends in CO_2 Capture/Separation Technologies: A Review, *Energy*, **46**: 431-441 (2012).

[10] Edali M., Idem R., Aboudheir A., 1D and 2D Absorption-Rate/Kinetic Modeling and Simulation of Carbon Dioxide Absorption Into Mixed Aqueous Solutions of MDEA And Pz in a Laminar Jet Apparatus, *Int. J. Greenhouse Gas Control*, **4**: 143-151 (2010).

[11] Van Krevelen D. W., Hoftijzer P. J., Huntjens F. J., Composition and Vapour Pressures of Aqueous Solutions of Ammonia, Carbon Dioxide and Hydrogen Sulfide, *Recueil*, **68**: 191-216 (1948).

[12] Van Krevelen D. W., Hoftijzer P. J, Applicability of the Results of Small-Scale Experiments to the Design of Technical Apparatus for Gas Absorption, *Trans. Inst. Chem. Eng.*, **32**: 60-67 (1954).

[13] Decoursey W. J., Thring R. W., Effects of Unequal Diffusivities on Enhancement Factors for Reversible and Irreversible Reaction, *Chem. Eng. Sci.*, **44:** 1715-1721 (1989).

[14] Decoursey W. J., Absorption with Chemical Reaction: Development of a New Relation for the Danckwerts Model, *Chem. Eng. Sci.*, **29**: 1867-1872 (1974).

[15] Decoursey W. J., Enhancement Factors for Gas Absorption with Reversible Reaction, *Chem. Eng. Sci.*, **37:** 1483-1489 (1982).

[16] Shen J., Yang Y., Maa J., Promotion Mechanism for CO_2 Absorption into Partially Carbonated Ammonia Solutions, *J. Chem. Eng. Japan*, **32**: 378-381 (1999).

[17] Last W., Stichlmair J., Determination of Mass Transfer Parameters by Means of Chemical Absorption, *Chem. Eng. Technol.*, **25:** 4-10 (2002).

[18] Ma'mun S., "Selection and Characterization of New Absorbents for Carbon Dioxide Capture", Ph.D Dissertation, Norwegian University of Science and Technology (2005).

[19] Van Krevelen D.W., Hoftijzer, P.J., Composition and Vapor Pressures of Aqueous Solutions of Ammonia, Carbon Dioxide and Hydrogen Sulfide, *Recueil*, **68**: 191-216 (1948).

[20] Roizard Ch., Wild G., Mass Transfer with Chemical Reaction: the Slow Reaction Regime Revisited, *Chem. Eng. Sci.*, **57**: 3479-3484 (2002).

[21] *Hikita* H., *Asai* S., Takatsuka T., Gas Absorption with a Two-Step Instantaneous Chemical Reaction, *Chem. Eng. J.*, **4**: 31-40 (1972).

[22] Olander D. R., Simultaneous Mass Transfer and Equilibrium Chemical Reaction, *AIChE J.*, **6**: 233–239 (1960).

[23] Onda K., Sada E., Kobayashi T., Fujine M., Gas Absorption Accompanied by Complex Chemical Reactions- I Reversible Chemical Reactions, *Chem. Eng. Sci.*, **25**: 753-760 (1970).

[24] Hung Ch-J., Kuo Ch-H., Mathematical Models for Mass Transfer Accompanied by Reversible Chemical Reaction, *AIChE J.*, **11**: 901–910 (1965).

[25] Ghaemi A., Torab-Mostaedi M., Ghannadi Maragheh M., Shahhosseini Sh., Kinetics and Absorption Rate Of CO_2 into Partially Carbonated Ammonia Solutions, *Chem. Eng. Comm.*, **198**: 1169-1181 (2011).

[26] Norouzbahari S., Shahhosseini Sh., Ghaemi A., CO_2 Chemical Absorption into Aqueous Solutions of Piperazine: Modeling of Kinetics and Mass Transfer Rate, *J. Natural Gas Sci. Eng.*, **26:** 1059-1067 (2015).

[27] Etemad E., Ghaemi A., Shirvani M., Rigorous Correlation for CO_2 Mass Transfer Flux in Reactive Absorption Processes, *J. Green. Gas Control*, **42**: 288–295 (2015).

[28] Yehia M., ElShazly S., The Use of Neural Network to Estimate Mass Transfer Coefficient from the Bottom of Agitated Vessel, *Heat Mass Transfer*, **51**: 465–475 (2015).

[29] Naeem S., Shahhosseini Sh., Ghaemi A., Simulation of CO_2 Capture Using Sodium Hydroxide Solid Sorbent in a Fluidized Bed Reactor by a Multi-Layer Perceptron Neural Network, *J. Natural Gas Sci. Eng.*, **31**: 305-312 (2016).

[30] Norouzbahari S., Shahhosseini Sh., Ghaemi A., Modeling of CO_2 Loading in Aqueous Solutions of Piperazine: Application of an Enhanced Artificial Neural Network Algorithm, *J. Natural Gas Sci. Eng.*, **24**: 18-25 (2015).

[31] Urata, S., Takada A., Murata J., Hiaki T., Sekiya A., Prediction of vapor–Liquid Equilibrium for Binary Systems Containing HFEs by Using Artificial Neural Network, *Fluid Phase Equilib.*, **199**: 63–78 (2002).

[32] Sözen A., Özalp M., Arcaklioğlu E., Calculation for the Thermodynamic Properties of an Alternative Refrigerant (R508b) Using Artificial Neural Network, *Appl Thermal Eng.*, **27**: 551-559 (2007).

[33] Jouyban, A., Majidi M.R., Jabbaribar F., Karim A.Z., Solubility Prediction of Anthracene in Binary and Ternary Solvents by Artificial Neural Networks (ANNs), *Fluid Phase Equilib.*, **225**: 133–139 (2004).

[34] Hagan, M.T., Demuth H.B., Beale M., "Neural Network Design", PWS Publishing Co. (1996).

[34] Haykin S., "Neural Networks a Comprehensive Foundation", McMaster University, Hamilton, Ontario, Canada(1994).

[35] Schalkoff, R.J., "Artificial Neural Networks", McGraw-Hill International Edition(1997).

[36] Bougie F., Iliuta M. C., CO_2 Absorption in Aqueous Piperazine Solutions: Experimental Study and Modeling, *J. Chem. Eng. Data*, **56**: 1547-1554(2011).

[37] Ghaemi A., Torab-Mostaedi M., Ghannadi Maragheh M., Shahhosseini Sh., Kinetics and Absorption rate of CO_2 into Partially Carbonated Ammonia Solutions, *Chem. Eng. Comm.*, **198**: 1169-1181(2011).

[38] Fu K., Chen G., Sema T., Zhang X., Liang Z., Idem R., Tontiwachwuthikul P., Experimental Study on Mass Transfer and Prediction Using Artificial Neural Network for CO_2 Absorption Into Aqueous DETA, *Chem. Eng. Sci.*, **100**: 195–202 (2013).

[39] Smith M., "Neural Networks for Statistical Modeling", Van Nostrand Reinhold, (1993).

[40] Demuth H., Beale M., "Neural Network Toolbox User's Guide", Copyright 1992-2002, The Math Works, Inc, Version 4, 840 (2000),

[41] Pangarkar V.G., Sharma M.M., Simultaneous Absorption and Reaction of Two Gases: Absorption of CO_2 And NH_3 in Water and Aqueous Solutions of Alkanol Amines, *Chem. Eng. Sci.*, **29**: 2297-2306 (1974).